

The azimuth moveout operator for anisotropic media

Tariq Alkhalifah¹

keywords: *dipmoveout, anisotropy*

ABSTRACT

The azimuth moveout (AMO) operator in homogeneous, moderate to strong, anisotropic media, like in isotropic media, has an overall skew saddle shape. Yet, the AMO operator in anisotropic media is complicated; it includes, among other things, triplications at low angles. Even, in weaker anisotropies, with anisotropy parameter $\eta=0.1$ (%10 anisotropy), the AMO operator differs from the isotropic one, though does not include triplications. The structure of the operator in VTI media (positive η) is stretched compared to operators in the isotropic media, with the amount of stretch dependent on the strength of anisotropy. If the medium is both $v(z)$ and anisotropic, a likely combination in practical problems, the shape of the operator again differs from that for isotropic media. Yet, the difference in the AMO operator for the homogeneous case and the $v(z)$ one is small even for anisotropic media. Simply stated, anisotropy impacts AMO more than typical smooth vertical velocity variations.

INTRODUCTION

The azimuth moveout (AMO) correction is a valuable tool for processing 3-D data. Most prestack imaging algorithms (i.e., dip moveout and prestack migration) are theoretically designed to work for data acquired along a single source-receiver azimuth. Yet, in 3-D surveys, data are seldom acquired along a single azimuth. Azimuth variation is often ignored and seismic traces are binned, after normal-moveout (NMO) correction, into a regularly sampled data set in offset and Common midpoint (CMP). Though, for isotropic homogeneous media, such binning has no bearing on reflections from horizontal events, ignoring the azimuth variation can harm reflections from dipping events (Biondi et al., 1998), resulting in the attenuation of such reflections when partial stacking is applied to reduce the volume of the data set (Hanson and Witney, 1995). Thus, the multi-azimuth nature of seismic data acquired using 3-D marine or land surveys, and the desire of processors to preserve energy from dipping events, made the AMO correction an important tool in processing.

¹**email:** tariq@sep.stanford.edu

Like the DMO operator, the AMO operator is applied after NMO correction. Because the AMO operator is small in size compared with the DMO operator, Alkhalifah and Biondi (1998) showed that smooth vertical velocity variation has an overall small influence on the operator shape. Strong vertical velocity variation was needed to considerably alter the shape of the homogeneous operator. The size of the residual AMO operator, which was smaller than the full AMO operator by a factor of 10, further demonstrated the fact that smooth $v(z)$ variations can some what be ignored in AMO correction.

Alkhalifah (1997c) showed that anisotropy can highly impact the 3-D DMO operator. In fact, for homogeneous media, the presence of anisotropy will give the DMO operator a 3-D shape. This is a big change from the 2-D operator associated with the isotropic DMO in homogeneous media. The presence of anisotropy also results in triplications in the DMO operator even for homogeneous media, where the DMO operator for the isotropic case has a simple ellipse shape. AMO consists of a cascade of a forward and inverse DMO. The inverse DMO is applied after rotating the axes by an angle equal to the desired azimuth correction. Thus, some of the features Alkhalifah (1997c) described for the DMO operator should apply to AMO operators, as well.

In this paper, I will investigate the impact that anisotropy has on AMO operators, specifically as it relates to the operator size and shape. The AMO operator for isotropic media will be used as a reference operator to judge the influence of anisotropy. Later, I will add vertical velocity variation to the mix, since the combination of velocity increase with depth and anisotropy is very common.

AZIMUTH MOVEOUT CORRECTION IN ISOTROPIC MEDIA

Azimuth moveout correction relies heavily on shape of the operator used in the application. Since these operators are convolved with the data their shapes and sizes may significantly influence the output of the operation. The time shift to be applied to the data is a function of the difference vector $\Delta\mathbf{m} = \Delta m(\cos \Delta\varphi, \sin \Delta\varphi)$ between the midpoint of the input trace and the midpoint of the output trace. The impulse response of the AMO operator in isotropic media has a general skewed saddle shape. In fact, for homogeneous isotropic media, the shape of the saddle is given by the following analytical equation

$$t_2(\Delta\mathbf{m}, \mathbf{h}_1, \mathbf{h}_2, t_1) = t_1 \frac{h_2}{h_1} \sqrt{\frac{h_1^2 \sin^2(\theta_1 - \theta_2) - \Delta m^2 \sin^2(\theta_2 - \Delta\varphi)}{h_2^2 \sin^2(\theta_1 - \theta_2) - \Delta m^2 \sin^2(\theta_1 - \Delta\varphi)}}, \quad (1)$$

where the offset vector of the input data is $\mathbf{h}_1 = h_1 \cos \theta_1 \mathbf{x} + h_1 \sin \theta_1 \mathbf{y} = h_1(\cos \theta_1, \sin \theta_1)$ and the offset vector of the desired output data is $\mathbf{h}_2 = h_2(\cos \theta_2, \sin \theta_2)$. The unit vectors \mathbf{x} and \mathbf{y} point respectively in the in-line direction and the cross-line direction, respectively. The traveltimes t_1 and t_2 are respectively the traveltime of the input

data after NMO has been applied, and the traveltime of the results before inverse NMO has been applied.

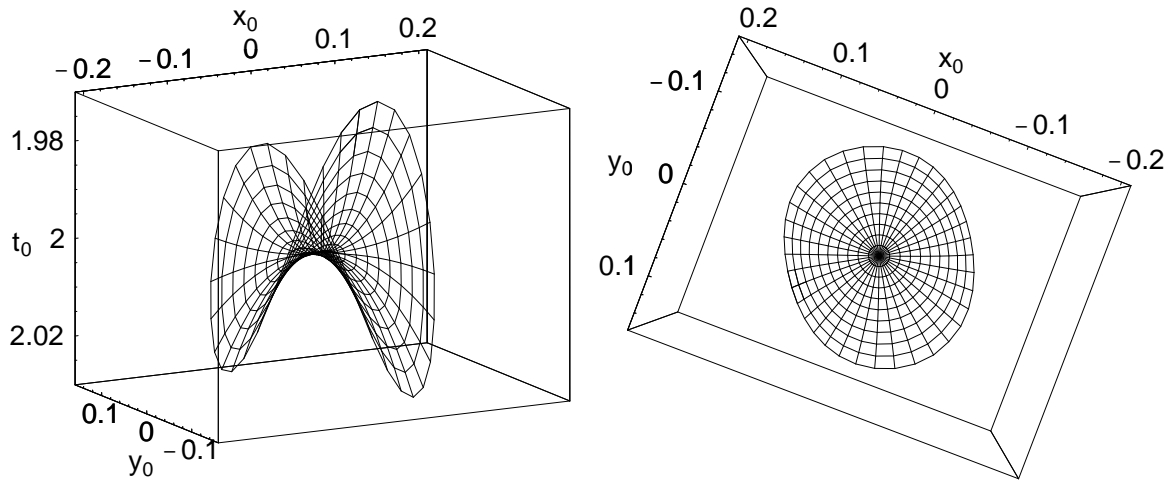


Figure 1: A side (left) and a top (right) view of the AMO operator for an isotropic homogeneous medium with an input and output offset of 2 km and correction to only the azimuth of 30 degrees. The x_0 (inline) and y_0 (crossline) axes are in km and the t_0 is in seconds. This holds here and throughout. The circular lines are contours of equal ray parameter. tariq1-AMO2eta0 [NR]

Figure 1 shows a side and a top view of the 30-degree correction AMO operator for an isotropic homogeneous medium. It is clearly 3-D in structure and has a general skewed saddle shape. The saddle is altered 30 degrees from the inline direction, in agreement with the amount of azimuth correction applied. The AMO operator domain has an overall circular shape. The shape of this AMO domain appears to be different from the one presented by Biondi et al. (1998) (a parallelogram), because I limit the zero-offset ray parameters when plotting the AMO operator.

Alkhalifah and Biondi (1998) generated AMO operators for isotropic $v(z)$ media. They used a nifty approach to build their AMO operators for $v(z)$ media. A similar approach is used here, but discussed below, to build the anisotropic AMO operators. Figure 2 shows a side and a top view of the 30-degree correction AMO operator for a $v(z)$ medium, in which velocity increase with depth linearly as $v(z) = 1.5 + 0.6z$ km/s, where z is the depth given in km. Again, the saddle is altered 30 degrees from the inline direction, in agreement with the amount of azimuth correction applied. The root-mean-square (rms) velocity for this model is similar to the homogeneous one and is equal to 2 km/s. Clearly, the $v(z)$ operator is very similar in shape and size to the homogeneous one, shown in Figure 1. Thus, Alkhalifah and Biondi (1998) concluded that the influence smooth velocity variations on the AMO operator is small.

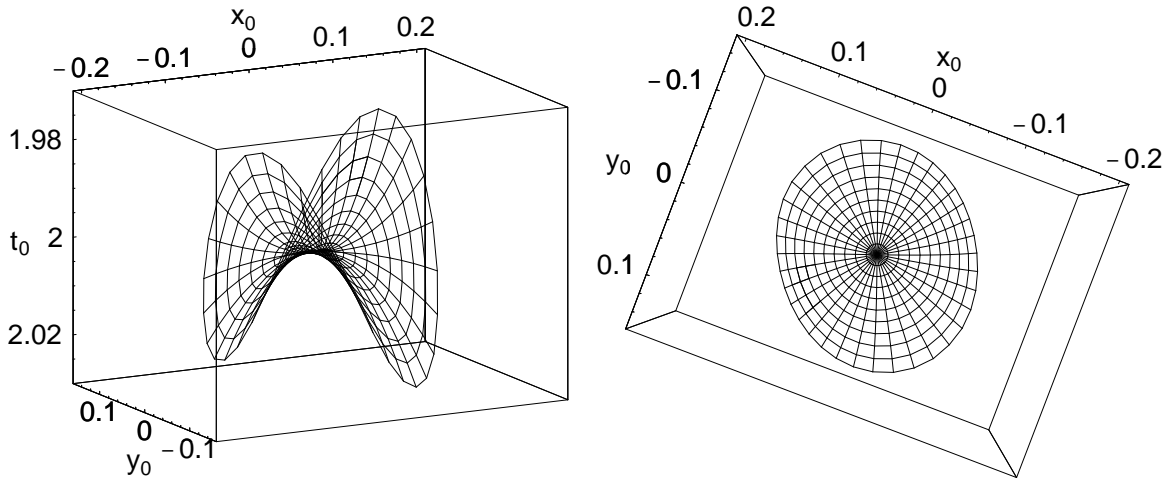


Figure 2: A side (left) and a top (right) view of the AMO operator for a linear $v(z)$ medium for an input and output offset of 2 km and correction to only the azimuth of 30 degrees. The linear velocity increase with depth is given by $v(z) = 1.5 + 0.6z$ km/s, which gives a root-mean-squared velocity of about 2 km/s at the input NMO corrected time of 2 s. tariq1-AMO2vzeta0 [NR]

ANISOTROPIC MEDIA PARAMETERIZATION

Here, I consider the simplest and probably most practical anisotropic model, that is a transversely isotropic (TI) medium with a vertical symmetry axis. Although, more complicated anisotropies can exist (i.e. orthorhombic anisotropy), the large amount of shales present in the subsurface makes the TI model the most influential on P-wave data (Banik, 1984).

In homogeneous transversely isotropic media with vertical symmetry axis (VTI media), P - and SV -waves (I omit the qualifiers in “quasi- P -wave” and “quasi- SV -wave” for brevity) can be described by the vertical velocities v_v and v_{sv} of P - and S -waves, respectively, and two dimensionless parameters ϵ and δ (Thomsen, 1986).

$$\epsilon \equiv \frac{c_{11} - c_{33}}{2c_{33}},$$

$$\delta \equiv \frac{(c_{13} + c_{44})^2 - (c_{33} - c_{44})^2}{2c_{33}(c_{33} - c_{44})}.$$

Tsvankin (1996) and Alkhalifah (1997b) demonstrated that P -wave velocity and traveltimes are practically independent of v_{sv} , even for strong anisotropy. This implies that, for practical purposes, P -wave kinematic signatures can be considered a function of just three parameters: v_v , δ , and ϵ .

Alkhalifah and Tsvankin (1995) further demonstrated that a new representation in terms of just *two* parameters is sufficient for performing all time-related processing,

such as normal moveout correction (including non-hyperbolic moveout correction, if necessary), dip-moveout removal, and prestack and post-stack time migration. These two parameters are the normal-moveout velocity for a horizontal reflector

$$v = v_v \sqrt{1 + 2\delta}, \quad (2)$$

and the anisotropy coefficient η ,

$$\eta \equiv 0.5 \left(\frac{v_h^2}{v^2} - 1 \right) = \frac{\epsilon - \delta}{1 + 2\delta}, \quad (3)$$

where v_h is the horizontal velocity. Since we are dealing here with time processing only two parameters will be used in this paper, v and η .

GENERATING THE AZIMUTH MOVEOUT OPERATOR IN VTI MEDIA

The AMO operator in anisotropic $v(z)$ media is constructed by cascading a forward and an inverse 3-D $v(z)$ DMO operators. An angular transformation, equal to the desired azimuth correction, is applied to the inverse operator. Therefore, to build the AMO operator we must first build the 3-D anisotropic $v(z)$ operator. Artley et al. (1993) suggested an approach to build a kinematically exact 3-D DMO operator in $v(z)$ media. Alkhalifah (1997c) used the same approach to build 3-D DMO operators in VTI $v(z)$ media. Following their approach, we construct the 3-D DMO operator by solving a system of six nonlinear equations to obtain six unknowns that include, among other things, the zero-offset time and surface position of the specular reflection point. The traveltimes are calculated and tabulated using a VTI $v(z)$ ray tracing. Because velocity varies only vertically, each ray propagating in the subsurface is contained in a vertical plane; therefore, 2-D raytracing is sufficient to calculate the traveltimes. The total traveltime is:

$$t_{sg} = t_s + t_g,$$

and therefore the gradient vector,

$$\nabla t_{sg} = \nabla t_s + \nabla t_g = \mathbf{p}_s + \mathbf{p}_g$$

has a direction that is normal to reflector dip. Because the zero-offset slowness vector \mathbf{p}_0 is also in the direction that is normal to reflector dip, then \mathbf{p}_0 is a scaled sum of the slownesses of the rays from the source \mathbf{p}_s and receiver \mathbf{p}_g to the specular point reflection. Therefore,

$$\mathbf{p}_0 = \lambda(\mathbf{p}_s + \mathbf{p}_g). \quad (4)$$

Considering the z-component gives

$$p_{0z} = \lambda(p_{sz} + p_{gz}),$$

then

$$\lambda = \frac{p_{0z}}{p_{sz} + p_{gz}}.$$

Since

$$\begin{aligned} p_{0z} &= \cos[\theta(p_0, t_0)]s(p_0, t_0), \\ p_{sz} &= \cos[\theta(p_s, t_s)]s(p_s, t_s), \end{aligned}$$

and

$$p_{gz} = \cos[\theta(p_g, t_g)]s(p_g, t_g),$$

where s is the slowness and θ is the phase angle, both of which are calculated using ray tracing and tabulated as a function of rayparameter p and the travelttime t . Then

$$\lambda = \frac{\cos[\theta(p_0, t_0)]s(p_0, t_0)}{\cos[\theta(p_s, t_s)]s(p_s, t_s) + \cos[\theta(p_g, t_g)]s(p_g, t_g)}. \quad (5)$$

Substituting equation (5) into the x - and y -components of equation (4) provides two of the six nonlinear equations needed to be solved. The other four equations are given by

$$0 = \xi(p_g, t_g) \cos \phi_g - \xi(p_s, t_s) \cos \phi_s + 2h \quad (6)$$

$$0 = \xi(p_g, t_g) \sin \phi_g - \xi(p_s, t_s) \sin \phi_s \quad (7)$$

$$0 = \tau(p_0, t_0) - \tau(p_s, t_s) \quad (8)$$

$$0 = \tau(p_0, t_0) - \tau(p_g, t_g), \quad (9)$$

Equation (6) is the requirement that the surface distances, ξ , along the inline component from both the source and receiver to the specular reflection point (SRP) add to equal the source-receiver offset, $2h$. Equation (7) is the requirement that the distances along the crossline component to the SRP are equal for the source and receiver. Equations (8) and (9) imply that the vertical times, τ from the source, the receiver, and the zero-offset surface positions to the SRP are equal. Both ξ and τ are calculated using ray tracing and then stored in a table as a function of ray parameter p and the travelttime t .

The inverse operator is calculated in the same way as the forward operator, but now we must calculate t_n or the total travelttime t_{sg} instead of t_0 , which is known. Subsequently, x_0 and y_0 are calculated in the same way as the forward approach.

To build the AMO operator, the output of the forward 3-DMO operator $t_0(t_n, p_x, p_y)$, $x_0(t_n, p_x, p_y)$, and $y_0(t_n, p_x, p_y)$ are inserted into the inverse 3-D DMO operator (another reference, Alkhalifah and Biondo,). Prior to applying the inverse operator the axes are rotated with an angle given by the desired azimuth correction. The result is an AMO operator given by

$$\begin{aligned} &t_{AMO}[t_0(t_n, p_x, p_y), p_x, p_y], \\ &x_{AMO}(t_n, p_x, p_y) = x_0(t_n, p_x, p_y) - x_0(t_0, p_x, p_y), \end{aligned}$$

and

$$y_{AMO}(t_n, p_x, p_y) = y_0(t_n, p_x, p_y) - y'_0(t_0, p_x, p_y),$$

where x'_0 and y'_0 correspond to the adjoint (inverse) operator in the rotated domain. The rotation angle is the azimuth correction angle. This is basically the same approach used by Alkhalifah and Biondi (1998) for isotropic $v(z)$ media. For anisotropic media, I use anisotropic ray tracing.

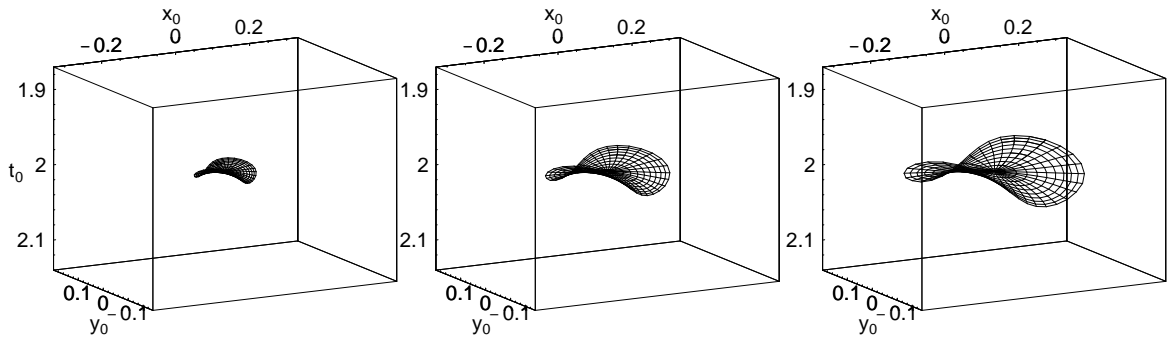


Figure 3: AMO operators for VTI homogeneous media for an input and output offset of 2 km and correction to only the azimuth. The azimuth corrections from left to right are 15, 30, and 45 degrees, respectively. The velocity is 2 km/s, $\eta=0.1$, and the input NMO corrected time is 2 s. tariq1-AMO3eta1ang [NR]

Figure 3 shows three AMO operators that correspond to three different azimuth correction angles in a VTI homogeneous medium. From left to right, the azimuth correction angles are 15, 30, and 45 degrees, respectively. The input and output offset are the same and equal to 2 km. Though these operators have a general saddle shape, they are different from their isotropic counterparts (Figure 1). They are considerably stretched and thus do not have the vertical size that the isotropic operators have. Additional differences will be apparent later when we take a closer look at the anisotropic operators. Though the general shape of the AMO operator is practically the same between the three azimuth corrections, the size is very much dependent on the amount of azimuth correction; the larger the azimuth correction the larger the AMO operator. Clearly, for zero azimuth correction the operator reduces to a point. The size dependence of the operator on azimuth holds regardless of the medium. The shape of the operator, however, is very much independent of azimuth correction. This phenomenon holds for homogeneous as well as $v(z)$ isotropic media (Alkhalifah and Biondi, 1998). As a result, we will, as Alkhalifah and Biondi (1998) did, use a single azimuth correction for most of the examples shown in this paper, that is a 30 degrees azimuth correction.

AMO OPERATORS IN VTI MEDIA

In homogeneous media, the presence of anisotropy results in a DMO operator that is 3-D in structure, and often includes triplications (Alkhalifah, 1997c). Since AMO is a combination of a forward and an inverse DMO, some of the anisotropic DMO operator features will appear in the AMO operator. The combination of anisotropy and vertical inhomogeneity should result in even more complicated AMO operators. The vertical velocity variation considered here is a linear one.

AMO in homogeneous media

In this section, We will look at three anisotropic models given by η equal 0.1, 0.2 and 0.3. Though, stronger anisotropy may exist, the majority of anisotropy in the subsurface conveniently lies within this range.

Figure 4 shows AMO operators for the first example, which is a homogeneous VTI medium with $\eta = 0.1$. The AMO operator corresponding to a pure offset correction, shown upper left, has a similar shape to the full 3-D DMO operator, shown lower-right, both concaved upward. The corresponding residual DMO operator for isotropic media is a purely 2-D operator. The azimuth-correction-only operator, shown upper right, differs from the isotropic-medium one shown in Figure 1. When the offset and azimuth corrections are combined in a single operator, it is given by the one shown in the lower left of Figure 4. The full DMO operator, shown in the lower-right, is clearly the largest in size. AMO operators that include offset correction alters the position of horizontal, as well as dipping, reflections. This alteration is necessary to correct for the non-hyperbolic moveout associated with VTI media for horizontal and dipping events.

Figure 5 shows a side and a top view of the AMO operator (shown in Figure 4 upper-right corner) that corrects for an azimuth of 30 degrees. The homogeneous medium has a $v=2$ km/s and $\eta=0.1$. The anisotropic AMO operator is clearly a stretched version of the isotropic one, shown in Figure 1. A similar stretch behavior exists in DMO operators in anisotropic media (Alkhalifah, 1997c). In addition, the presence of anisotropy has altered the shape of the AMO operator. This is more evident on the top view, where the circular shape of the isotropic AMO operator is becoming more rectangular in anisotropic media. These changes in the AMO operator due to anisotropy is clearly larger than the ones associated with smooth (linear in this case) vertical velocity variation (Figure 2). Thus, anisotropy can pause a bigger problem to the conventional AMO than vertical velocity variation.

A stronger anisotropy (Figure 6), with $\eta=0.2$, causes the AMO operator to stretch even more. It also results in triplications that takes place at moderate dip angles. A closer look, given by the inline and crossline components of the AMO operator (Figure 7), reveals such triplications in detail. These triplications exist in both the inline and crossline components of the AMO operator, as well as, all angles in between.

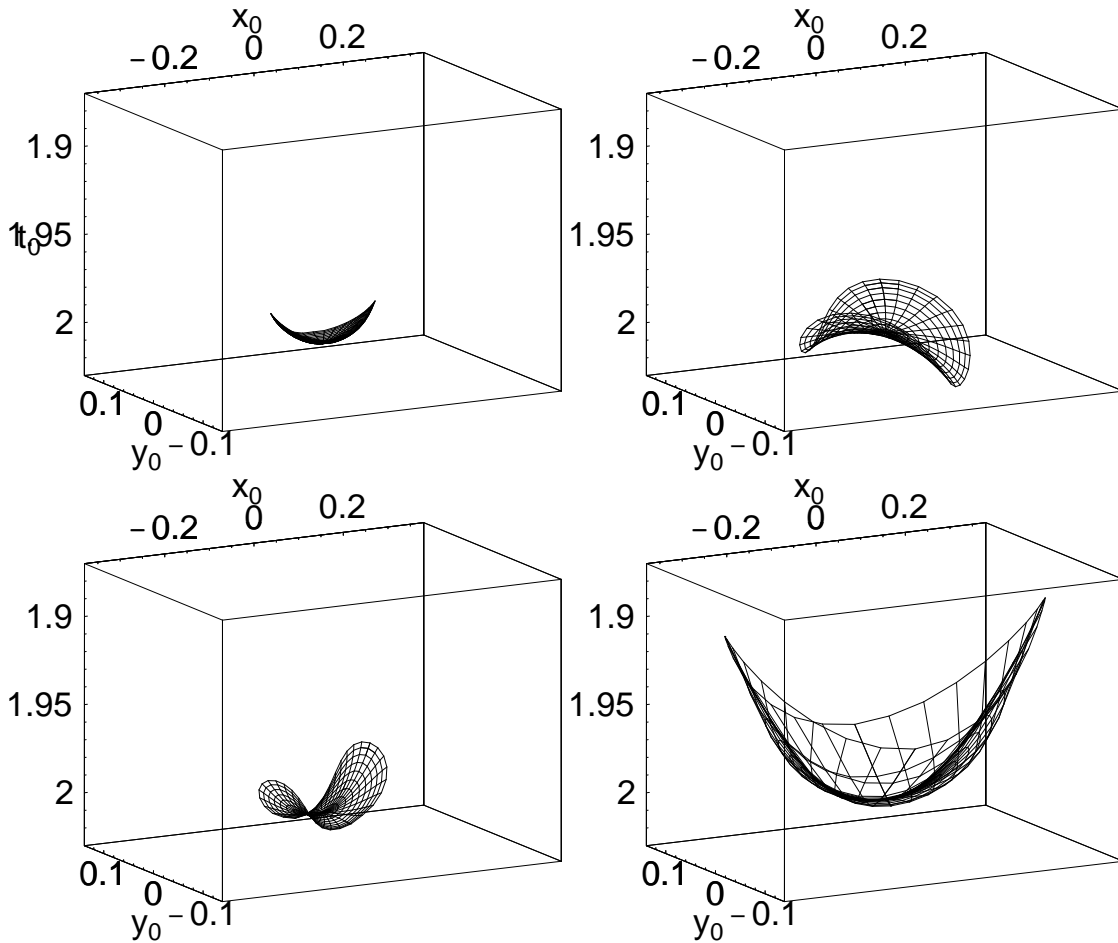


Figure 4: Four AMO operators in homogeneous VTI media, with $\eta = 0.1$ and $v = 2.0$ km/s. The upper left operator corresponds to a correction in offset only, or residual DMO, the upper right operator corresponds to a correction in azimuth only, the lower-left corresponds to a correction in both offset and azimuth, while the lower-right operator is the 3-D VTI DMO operator. The offset correction, used in all the examples, is from 2.0 km to 1.5 km. The correction in azimuth as previously stated is 30 degrees. tariq1-AMO4eta1 [NR]

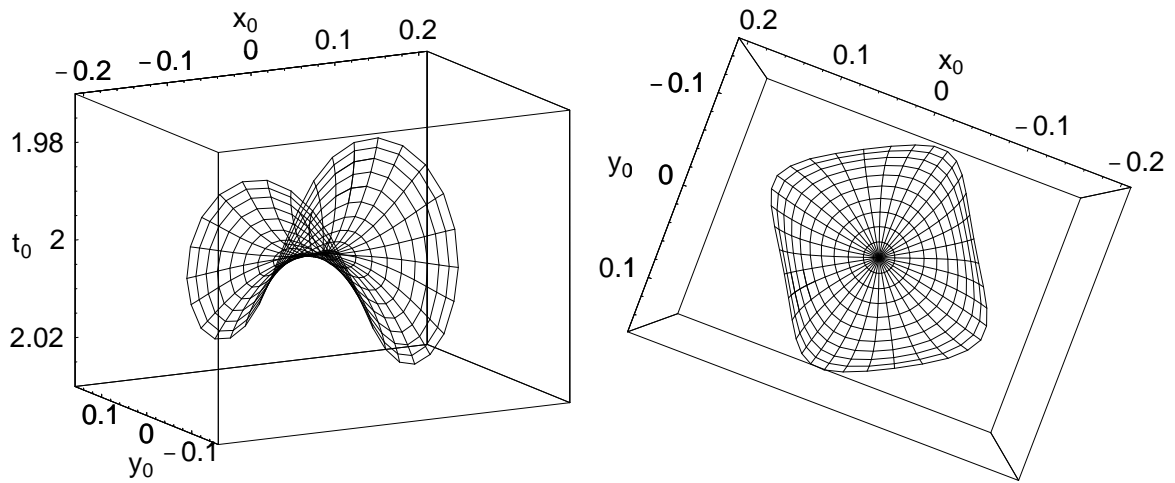


Figure 5: A side (left) and a top (right) view of the AMO operator for a VTI homogeneous medium for an input and output offset of 2 km and correction to only the azimuth of 30 degrees. The medium has $v=2$ km/s and $\eta=0.1$. tariq1-AMO2eta1 [NR]

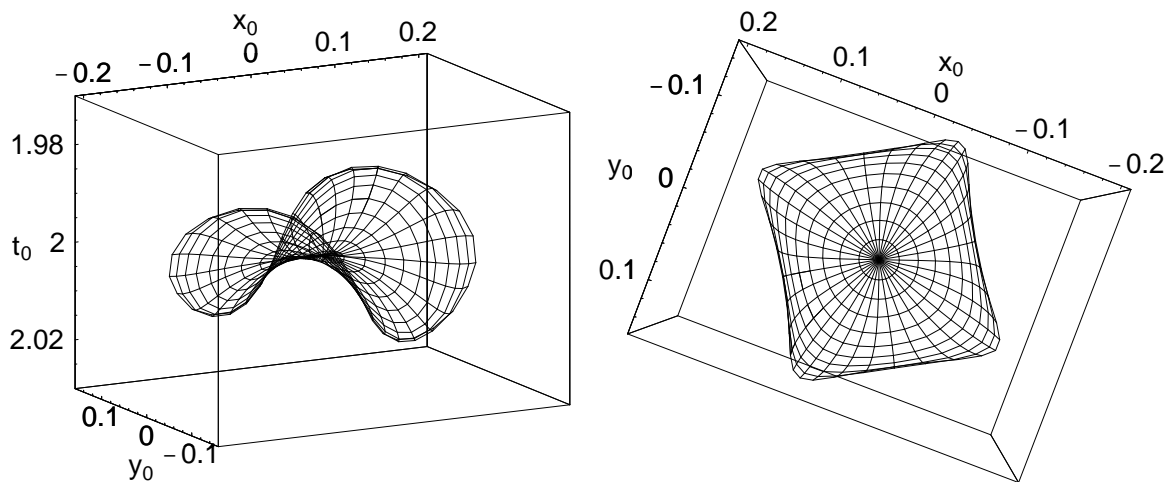


Figure 6: A side (left) and a top (right) view of the AMO operator for a VTI homogeneous medium for an input and output offset of 2 km and correction to only the azimuth of 30 degrees. The medium has $v=2$ km/s and $\eta=0.2$. tariq1-AMO2eta2 [NR]

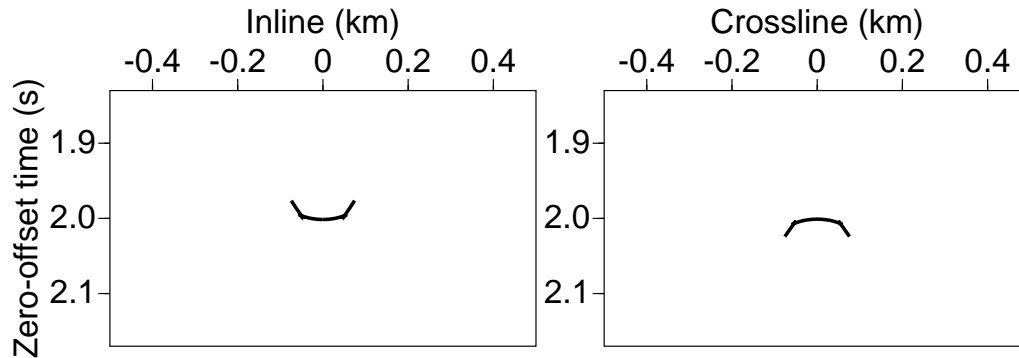


Figure 7: The inline and crossline components of the AMO operator (or residual DMO) in Figure 6, but with a wider aperture which includes the triplications. This operator, as previously stated, applies only an azimuth correction of 30 degrees. `tariq1-incrossanis30eta0.2` [NR]

Figure 8 shows AMO operators for an even stronger anisotropy with $\eta = 0.3$, and same velocity used previously. The AMO operator corresponding to a pure offset correction, shown upper left, again has a similar shape to the full 3-D DMO operator, shown lower-right, which is generally concaved upward. The crossline component of this operator is mainly the result of anisotropy. Recall that the corresponding residual DMO operator for isotropic media is a purely 2-D operator. The size of this out-of-plane component is greater for this strong anisotropy model than that for $\eta=0.1$ (Figure 4 upper-left corner), and therefore the size of the crossline component is dependent on the strength of anisotropy. The same observation holds for DMO operators, shown lower-right corners of Figures 4 and 8. The azimuth-correction-only operator, shown upper right, differs considerably from the isotropic-medium one shown in Figure 1. When the offset and azimuth corrections are combined in a single operator, it is given by the one shown in the lower left of Figure 8, and it is simply given by the convolution of the offset operator (upper-left) and the azimuth operator (upper-right).

Figure 9 shows a side and a top view of the AMO operator (shown in Figure 8 upper-right corner) that corrects for an azimuth of 30 degrees. The homogeneous medium has $v=2$ km/s and $\eta=0.3$. Again, the same conclusions hold here with regard to the impact of anisotropy on the AMO operator, which is obviously stronger than the impact of the smooth vertical velocity variation, given by Figure 2. Clearly, this operator is very different from the isotropic one; the anisotropic operator is stretched and has a more rectangular shape.

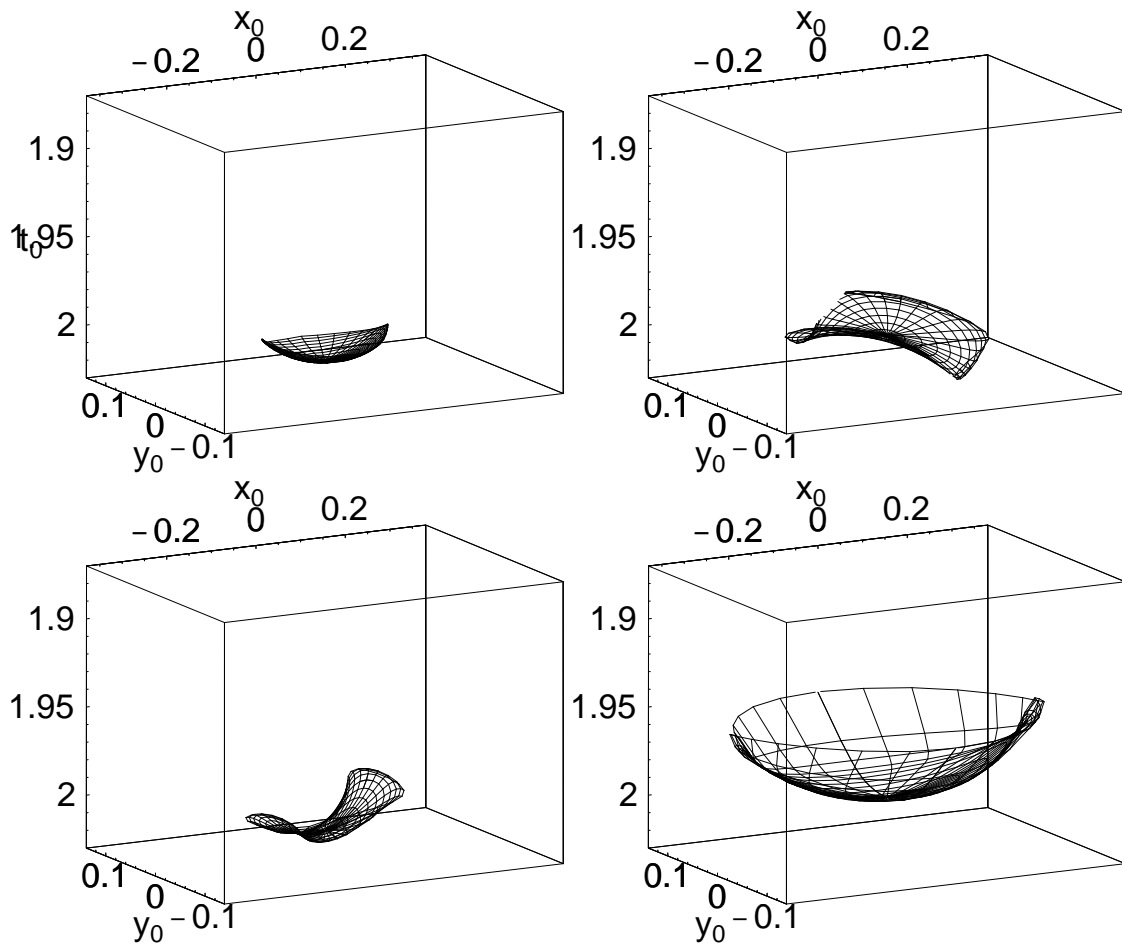


Figure 8: Four AMO operators in homogeneous VTI media, with $\eta = 0.3$ and $v = 2.0$ km/s. The upper left operator corresponds to a correction in offset only, or residual DMO, the upper right operator corresponds to a correction in azimuth only, the lower left corresponds to a correction in both offset and azimuth, while the lower right operator is the 3-D VTI DMO operator. tariq1-AMO4eta3 [NR]

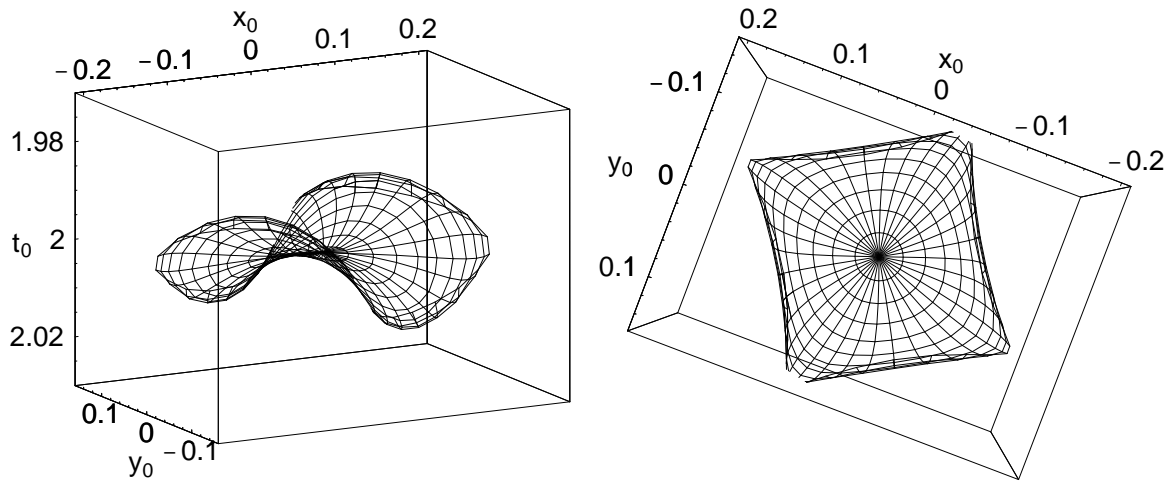


Figure 9: A side (left) and a top (right) view of the AMO operator for a VTI homogeneous medium for an input and output offset of 2 km and correction to only the azimuth of 30 degrees. The medium has $v=2$ km/s and $\eta=0.3$. tariq1-AMO2eta3 [NR]

AMO in vertically inhomogeneous media

The $v(z)$ modal used here is a linear one with velocity given by $v(z) = 1.5 + 0.6z$ km/s. This model is a good representation of many locations in the subsurface, including the Gulf of Mexico.

Figure 10 shows a side and a top view of the AMO operator that corrects for an azimuth of 30 degrees. The VTI medium has $\eta=0.1$. The anisotropic AMO operator is clearly a stretched version of the isotropic one, shown in Figure 2. This operator is very similar to the homogeneous medium one (Figure 5), which clearly suggests that the impact of $v(z)$ velocity variation on the operator is small. It also implies that the homogeneous VTI AMO operator can be used to successfully correct for data from $v(z)$ VTI media.

The same observations hold for even stronger anisotropy given by $\eta = 0.3$. Figure 11 shows such an operator where clearly the shape of the operator is different from the isotropic one. Such strong anisotropy changes the shape of the AMO operator considerably. Also, the operator is very similar to the homogeneous medium one (Figure 9), again suggesting that the influence of such smooth vertical velocity variation is small on the AMO operator, even for such a strong anisotropy.

In summary, AMO operators in $v(z)$ media are very similar to their homogeneous media counterparts, granted that the strength of anisotropy is the same. If the anisotropy strength changes between the models the AMO operator shape can change, as well. Anisotropy can cause triplications in the operator even at low angles.

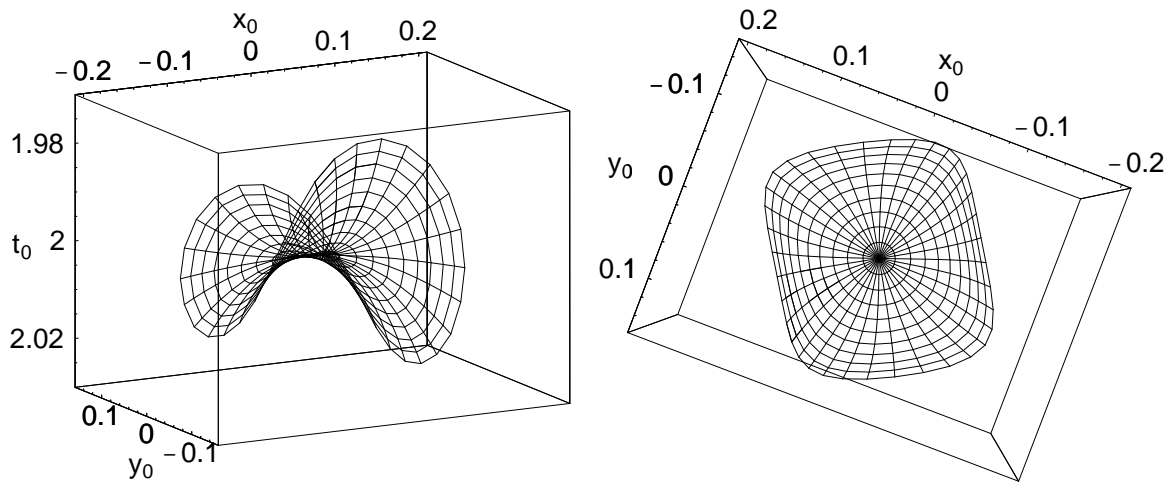


Figure 10: A side (left) and a top (right) view of the AMO operator for a VTI vertically inhomogeneous medium for an input and output offset of 2 km and correction to only the azimuth of 30 degrees. The medium has $v = 1.5 + 0.6z$ km/s and $\eta=0.1$. `tariq1-AMO2vzeta1` [NR]

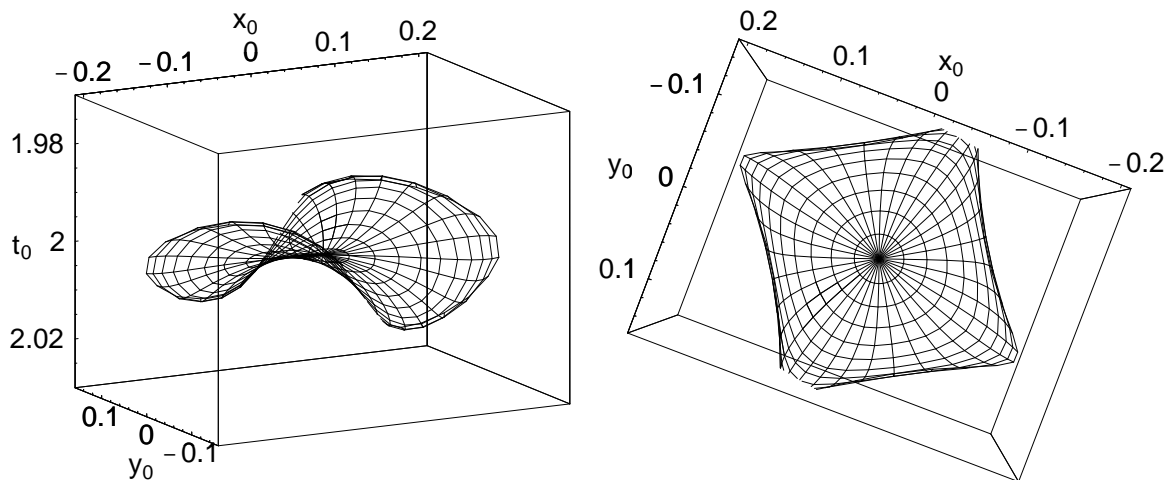


Figure 11: A side (left) and a top (right) view of the AMO operator for a VTI vertically inhomogeneous medium for an input and output offset of 2 km and correction to only the azimuth of 30 degrees. The medium has $v = 1.5 + 0.6z$ km/s and $\eta=0.3$. `tariq1-AMO2vzeta3` [NR]

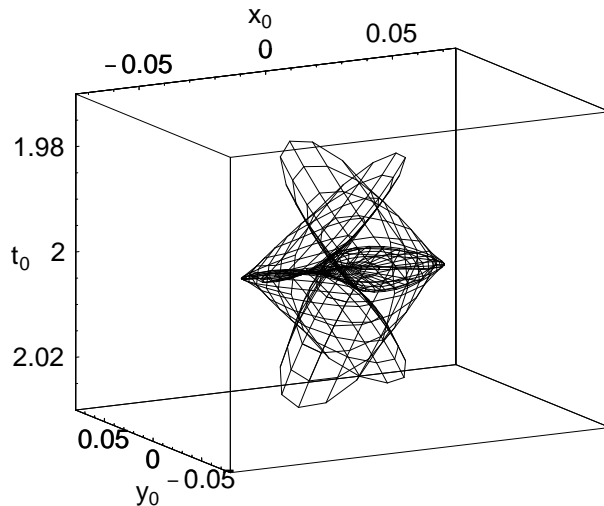
RESIDUAL AMO OPERATORS

The residual AMO operator includes a cascade of two AMO operators corresponding to the same correction, but opposite sign, in offset and azimuth, but with different media parameters. Equivalently, it includes four 3-D $v(z)$ DMO operations; two forward operations and two inverse ones. The difference between each of the pair of forward and inverse operations is the medium parameters. In this case, a pair of forward and inverse DMO's, or AMO, is applied for an isotropic medium followed by another pair corresponding to a VTI medium.

The size of the residual AMO operator is directly dependent on the amount of medium perturbation from the isotropic background model. The residual operator provides information on the impact that the perturbation in anisotropy has on the AMO operator. The smaller the size of the residual operator, the lesser the anisotropy has influenced the AMO operator, and thus the lesser the need to use it.

Figure 12 shows the residual AMO operator that corrects an isotropic AMO operator to a VTI AMO one. In other words, this residual AMO operator, when convolved with the isotropic-medium AMO operator, provides us with the VTI AMO operator. The AMO operators involved correspond to a pure azimuth correction of 30 degrees. The resulting residual operator is, as expected, smaller than the corresponding full AMO operator shown in Figure 5. The shape of the operator is rather complicated with triplications at low angles.

Figure 12: A side view of a residual AMO operator responsible for the correction from a VTI model to an isotropic one for a pure azimuth correction of 30 degrees. The anisotropy model considered here has $\eta = 0.1$ and $v = 2$ km/s. tariq1-AMO1eta1res [NR]



A better view of the operator in Figure 12 can be obtained by displaying the inline and crossline components of the residual AMO operator, separately. Figure 13 shows such a display, which confirms the low angle nature of the triplication and the small size of the operator. Thus the differences in the AMO operator for homogeneous and VTI media starts at a considerably low angle.

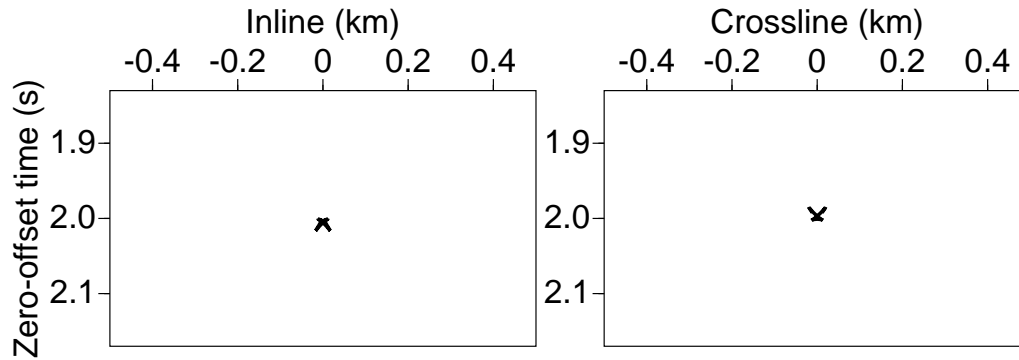


Figure 13: The crossline and inline components of the residual AMO operator shown in Figure 12. `tariq1-incross30anis1res` [NR]

REAL DATA EXAMPLE

Alkhalifah (1997a) extracted anisotropy parameters from field data from offshore Angola. These parameters, when used to migrate the data, result in improved images of the subsurface, including better fault reflection focusing. Since, the data set corresponds to a 3-D marine survey, with some source-receiver azimuth variations in the original data, the application of AMO might improve the data. Using the inverted anisotropic parameters, I will generate AMO operators applicable to this data set, and compare these operators with the conventional isotropic homogeneous-medium operator.

Figure 14 shows the anisotropic parameters extracted from the Angola data set. Clearly, the level of anisotropy in Angola, given by these parameters, is strong. Figure 15 shows a side and a top view of the AMO operator that resulted from the parameter in Figure 14, corresponding to a correction only to azimuth of 30 degrees. The input NMO-corrected time for the operator is 2.5 s. The operator, as expected from such a strong anisotropy, has triplications and has a somewhat complicated shape. Such triplications can be seen more clearly in Figure 16, which shows the inline and crossline components of the operator in Figure 15, separately. Most of the complications in the operator arise from the anisotropy in the medium, not the vertical inhomogeneity. As evidence, Figure 17 shows the 30-degree azimuth correction operator corresponding to an isotropic $v(z)$ medium, with velocity given by Figure 14 (left). The operator, absent anisotropy, looks very similar to the conventional operator for isotropic homogeneous media.

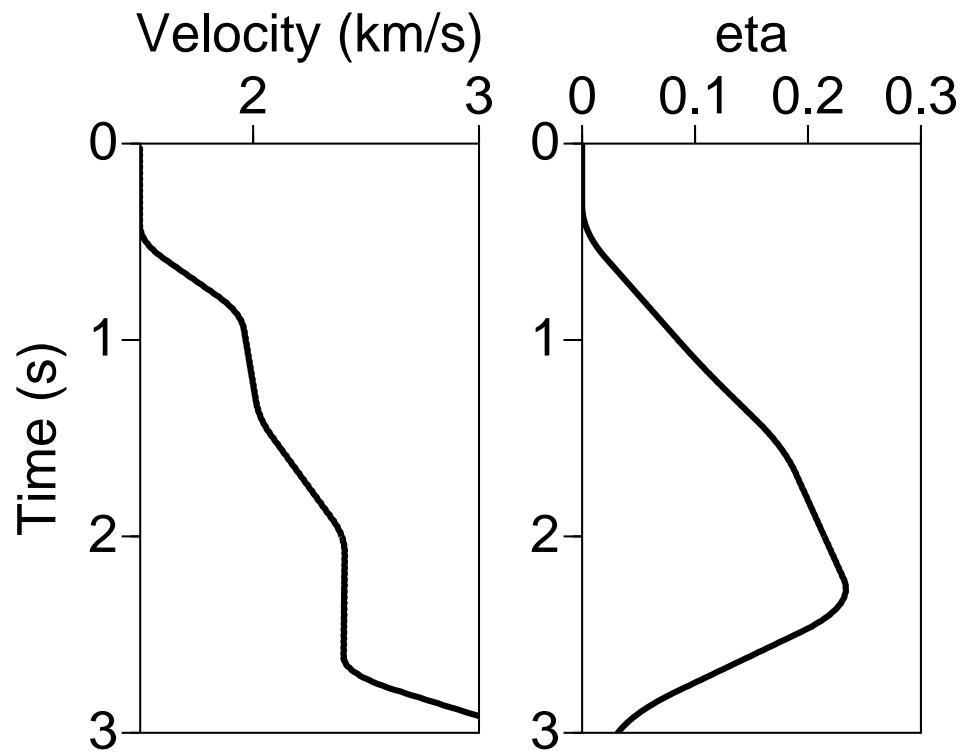


Figure 14: Curves of the interval NMO velocity and η extracted from the Angola data (Alkhalifah, 1997a). `tariq1-veta` [NR]

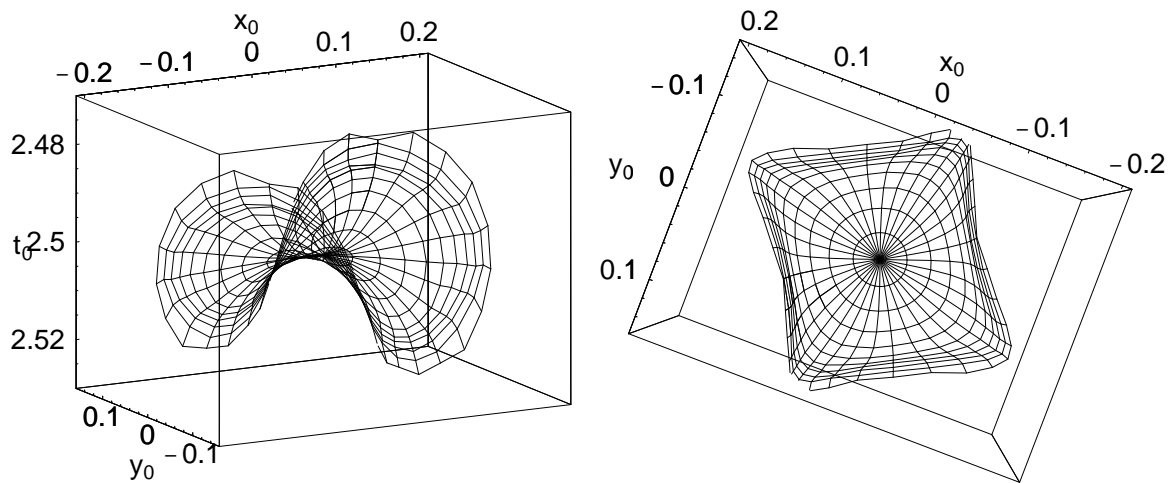


Figure 15: A side (left) and a top (right) view of the AMO operator for a VTI vertically inhomogeneous medium for an input and output offset of 2 km and correction to only the azimuth of 30 degrees. The medium is characterized by the velocity and η shown in Figure 14. `tariq1-AMO2field` [NR]

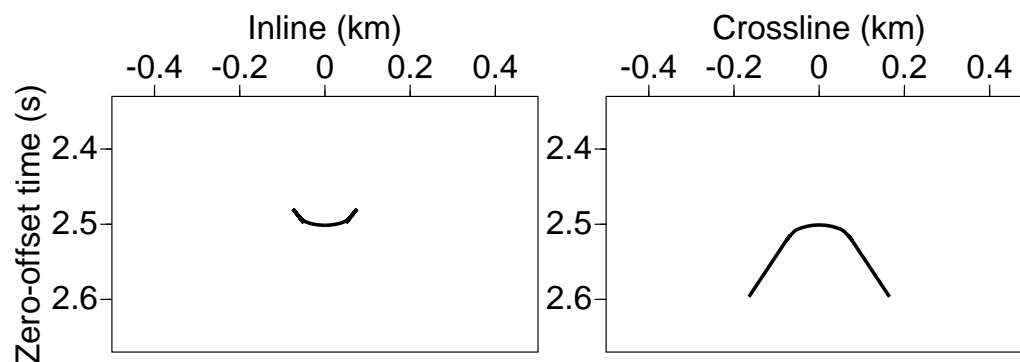


Figure 16: The inline and crossline components of the AMO operator (or residual DMO) in Figure 15, but with a wider aperture which includes the triplication. This operator, as previously stated, applies only an azimuth correction of 30 degrees. `tariq1-incrossanis30field` [NR]

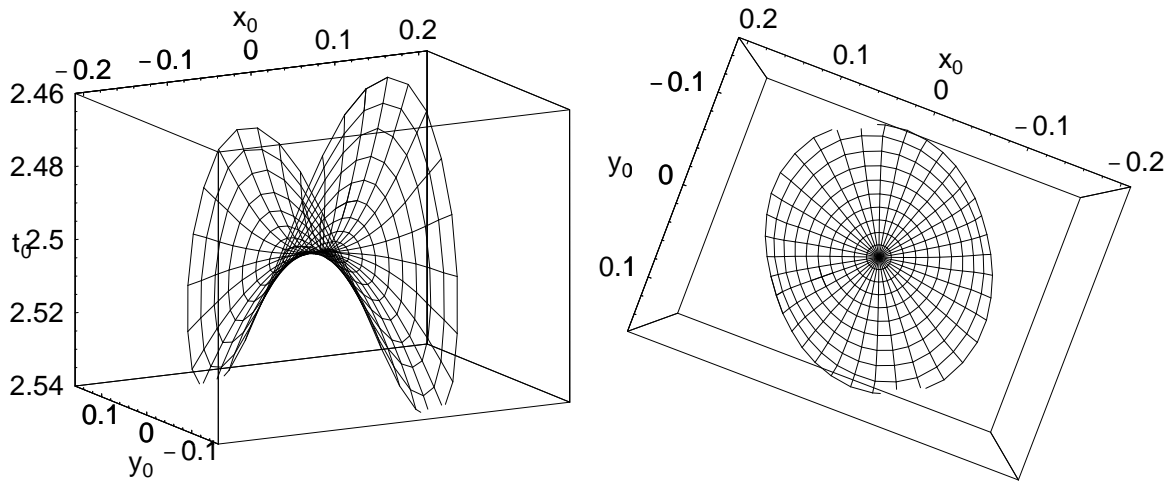


Figure 17: A side (left) and a top (right) view of the AMO operator for an isotropic vertically inhomogeneous medium for an input and output offset of 2 km and correction to only the azimuth of 30 degrees. The medium is characterized by the velocity curve shown in Figure 14. `tariq1-AMO2fieldvz` [NR]

CONCLUSIONS

For moderate and strong anisotropy, the AMO operator has a shape and size that differs considerably from the AMO operator in isotropic media. Yet the general shape of the operator for all media remains overall a skewed saddle. The difference between the isotropic and anisotropic AMO operators is noticeable even for weak anisotropy. This behavior is fundamentally different from what Alkhalifah and Biondi (1998) observed for media with vertical velocity variation. Smooth $v(z)$ hardly alters the shape or size of the homogeneous AMO operator. Thus, the impact of anisotropy on AMO is greater than the impact of $v(z)$, even more so than what Alkhalifah (1997c) showed for DMO. The insignificance of smooth velocity variation holds for anisotropic media as well.

REFERENCES

- Alkhalifah, T., and Biondi, B., 1998, The azimuth moveout operator for vertically inhomogeneous media: *SEP-97*, 95–116.
- Alkhalifah, T., and Tsvankin, I., 1995, Velocity analysis for transversely isotropic media: *Geophysics*, **60**, 1550–1566.
- Alkhalifah, T. A., 1997a, Seismic data processing in vertically inhomogeneous TI media: *Geophysics*, **62**, 662–675.

- Alkhalifah, T., 1997b, Acoustic approximations for seismic processing in transversely isotropic media: accepted for *Geophysics*.
- Alkhalifah, T., 1997c, Kinematics of 3-d dmo operators in transversely isotropic media: *Geophysics*, **62**, 1214–1219.
- Artley, C., Blondel, P., Popovici, A. M., and Schwab, M., 1993, Equations for three dimensional dip moveout in depth-variable velocity media: *SEP-77*, 43–48.
- Banik, N. C., 1984, Velocity anisotropy of shales and depth estimation in the north sea basin: *Geophysics*, **49**, no. 9, 1411–1419.
- Biondi, B., Fomel, S., and Chemingui, N., 1998, Azimuth moveout for 3-d prestack imaging: *Geophysics*, **63**, 574–588.
- Hanson, D. W., and Witney, S. A., 1995, 3-D prestack depth migration – velocity model building and case history: 1995 Spring Symposium of the Geophys. Soc. of Tulsa, Soc. Expl. Geophys., *Seismic Depth Estimation*, 27–52.
- Thomsen, L., 1986, Weak elastic anisotropy: *Geophysics*, **51**, no. 10, 1954–1966.
- Tsvankin, I., 1996, P-wave signatures and notation for transversely isotropic media: An overview: *61*, **2**, no. 467-483.